Triplet exciton fine structure in Pt-rich polymers studied by circularly polarized emission under high magnetic field

Chuang Zhang, Dali Sun, Ryan McLaughlin, Dmitry Semenov, Stephen McGill, Zhi-Gang Yu, Eitan Ehrenfreund, and Zeev Valy Vardeny

Phys. Rev. B **98**, 155205 — Published 23 October 2018

DOI: 10.1103/PhysRevB.98.155205

Triplet exciton fine structure in Pt-rich polymers studied by circularly polarized emission under high magnetic field

Chuang Zhang[1], Dali Sun[1,†], Ryan McLaughlin[1], Dmitry Semenov[2], Stephen McGill[2], Zhi-Gang Yu[3], Eitan Ehrenfreund[4], Zeev Valy Vardeny[1,*]

[1]*Department of Physics and Astronomy, University of Utah, Salt Lake City, UT 84112, USA*

[2]*National High Magnetic Field Laboratory, Tallahassee, FL 32310, USA*

[3]*SP/ Applied Sciences Laboratory, Washington State University, Spokane, WA, 99210, USA*

[4]*Physics Department and Solid State Institute, Technion-Israel Institute of Technology, Haifa 32000, Israel*

Incorporating heavy atoms into polymer chains represents an effective way to generate emissive triplets. Here we used magneto-optical emission spectroscopy up to 17.5 Tesla for studying the fine structure of the triplet exciton in a series of Pt-rich π-conjugated polymers with various intrachain Pt concentrations. We found that their phosphorescence emission band shows substantial field-induced circular polarization (FICPO) up to 50% with an unusual, non-monotonic field dependence at cryogenic temperature. From the field-induced energy splitting between left and right circularly polarized phosphorescence we obtained the effective g factor of triplet exciton varying in the range of -0.13 to 0.85, which depends on the Pt concentration in the polymer chains. The FICPO of triplet emission originates from the population difference in spin sublevels, which is determined by thermal equilibrium subjected to spin-orbit coupling (SOC), exchange and Zeeman interactions. Surprisingly we also observed FICPO in the fluorescence emission that results from the singlet-triplet interaction caused by the strong SOC. From these results we could extract the various interaction parameters that describe the exciton fine structure in these Pt-contained compounds.

*Corresponding author: val@physics.utah.edu.

[†]Present address: Department of Physics, North Carolina State University, Raleigh, NC 27695, USA

I. INTRODUCTION

Optical transitions of spin-polarized electronic states are usually associated with the absorption and/or emission of circularly polarized light, as previously observed in traditional III-V semiconductors (e.g., GaAs).[1] When an external magnetic field is applied to such compounds, the energy splitting between the spin-polarized states is reflected in the separation of left- and right-circular polarized absorption/emission bands.[2] This phenomenon has been investigated for measuring the Landé *g*-factor and profile the fine structure of the luminescent excitons in semiconductor quantum dots[3,4] and quantum wells.[5,6] By comparison, the excitons in organic semiconductors are more localized than in the inorganic semiconductors, and thus they are treated as Frenkel (and/or charge-transfer) excitons that are spin½ e-h pairs in singlet or triplet configurations. The triplet exciton with spin quantum number, S=1 is naturally susceptible to the Zeeman interaction and shows energy splitting upon the application of magnetic field.[7-9] The fine structure of triplet exciton in organic semiconductors has been determined by optically detected magnetic resonance. This becomes less effective in materials that show extremely short spin lifetime caused by strong spin-orbit coupling (SOC).[10,11] The strong SOC also results in luminescent triplet in the form of phosphorescence, which may show field induced circularly polarized emission that may be useful for studying the triplet exciton fine structure.[12-14]

Usually circularly polarized optical transitions in organic compounds have been considered in chiral molecules,[15-19] in which the spin splitting is intrinsic according to the specific underlying molecular structure[20], and thus cannot be well-controlled by applying external magnetic field. However organic complexes that contain heavy metal atoms have been widely used as triplet emitters in organic light emitting diodes,[21] As such the phosphorescence from the triplet states could be influenced by applying external magnetic field.[22,23] As an important type of triplet emitters, the Pt-rich organic compounds shows metal-to-ligand charge-transfer (MLCT) excitons comprising of an electron localized mostly on the Pt metal atom (5d orbital) and a hole localized on the organic ligand (π bond).[24] The sizable electron-hole exchange interaction differentiates between the spin triplet excitons (TE) that lie lower in energy than the spin singlet excitons (SE). Interestingly since the Pt-rich compounds possess intermediately strong

SOC,[25,26] both TE and SE generate substantial photoluminescence which may be susceptible to field-induced circular polarization (FICPO). Thus magneto-optical studies on the photoluminescence emission would be very helpful for probing the exciton fine structure in these triplet emitters,[27] as well as optically reading/writing spin states towards spintronics applications.[28-30]

Here we performed magneto-optical investigations on Pt-rich π-conjugated polymers. In these compounds the heavy Pt atoms are intrachain and thus causes relatively strong effective SOC which mixes the SE and TE wave functions, thereby substantially increasing both the intersystem crossing rate (SE→TE) and the optical transition probability from the TE to the singlet ground state, S_0.[24,25] As a result, the phosphorescence (PH) emission from the TE becomes allowed and may be even stronger than the fluorescence (FL) emission from the SE. In fact the SE→TE intersystem crossing time in Pt-polymers was measured to range from 3 to 10 ps,[25] and thus there is only a small amount of radiative SE in the form of FL emission during this time interval. In addition, the chemical versatility of these polymers allows us to modify the Pt abundance in the chain that modifies the effective SOC, which, in turn modifies the TE spin sublevels and the optical transitions.

To analyze the FICPO phenomenon we recall that electric dipole related optical transitions leave the spin angular momentum ($\hbar S_z$) unchanged; whereas the orbital angular momentum along the photon propagation direction ($\hbar L_z$) is changed by $\pm\hbar$. Consequently, when the excited state structure becomes asymmetric with respect to the spin sense of emitted photon due to the magnetic field interaction, an energy splitting occurs between two almost degenerate excited states that induces circularly polarized emission.[31] However the TEs spin states in the organics are not degenerate, but show fine structure which dominates at zero magnetic field. Usually the fine structure is caused by the e-h dipole and/or exchange couplings, known as the zero field splitting (ZFS) parameters.[11] This would suppress the FICPO effect in the PH emission at low field, since the fine structure may be larger than the Zeeman interaction. In addition, when the field is applied in an arbitrary direction with respect to the molecular principal axis, the

energy splitting of the TE sublevels would vary with the field direction, and this would further suppress the measured FICPO in the PH emission in randomly oriented films.

In this work, we present the FICPO response of both FL and PH emissions in a series of Pt-rich π-conjugated polymers with varying intrachain Pt concentration which shows the important role of SOC in the spin-related optical transitions from this class of organic semiconductors. We found that the induced circular polarization (CP) of the PH emission in the most Pt-rich polymer is ~4% at magnetic field B=17.5 T, and the effective g-value substantially deviates from that of the free electron (g_e=2.002). The obtained FICPO response, CP(B), is not monotonic with B especially at large fields, showing that the exciton fine structure and the SOC dominate the spin sublevel energies. Interestingly, the CP(B) response of the primary 0-0 band (denoted hereafter as the "P band"), the so-called super-phosphorescence band,[32] is different from that of the vibronic PH side bands (denoted hereafter as the "V band"); this is caused by the TE-TE coherence that is unique to the P band of Pt polymers. Unexpectedly FICPO related to the FL band was also observed in one of these polymers, which indicates that the SE is also subjected to the SOC through the SE-TE interaction in the Pt-contained systems.

II. EXPERIMENTAL RESULTS

The Pt-rich polymers used here contain Pt-$(PBu_3)_2$ moieties separated by different length π-conjugated spacers, as shown in Fig. 1a (denoted as Pt-1, Pt-3 and Pt-Q).[26] For the high-field FICPO measurement (Fig. 1b), the Pt-polymer film was placed in a liquid helium cryostat (T=4 K), and excited with a 405 nm continuous-wave diode laser from the substrate side using an optical fiber attached to the sample holder. The light emission from the film was collected in free space by an optical lens placed parallel to the film in the cryostat. The magnetic field, B was provided by a 17.5 T superconducting magnet (NHMFL, SCM-3). The setup was designed to be in the Faraday configuration (B parallel to the light propagation direction), with the film normal along the B direction. The collected light emission passed through an optical window followed by a broadband quarter-wave plate (400 to 800 nm, Thorlabs) and a linear polarizer, which were used to separate the left (L, having intensity I_L) and right (R, having intensity I_R) circularly polarized components (See experimental details in ref.33). The L/R emissions were thus

measured using a fiber spectrometer (Ocean Optics, USB4000-ES), and the CP value in the light emission is defined as $\rho=(I_R-I_L)/(I_R+I_L)$.

The emission spectra from the three Pt-rich polymers are shown in Fig. 1c. In Pt-1 we identify the sharp band centered at ~523 nm as the primary PH band (P band), which according to previous study[24] is attributed to super-PH. At longer wavelengths there appears a series of vibronic side bands (V band) with a prominent peak centered at ~571 nm. The PH emission from the TE state is allowed due to the SOC that mixes the photoexcited SE with the TE. In Pt-3 the P and V bands are also clearly observed in the PH emission, but red-shifted to ~580 nm and 614 nm, respectively. In addition, a weak FL band appears at ~485 nm which agrees with the previous report.[25] The weakness of the FL emission in the spectrum is a direct consequence of the SE→TE intersystem crossing time, τ_{ISC}, where the shorter is τ_{ISC} the shorter is the allowed time for the FL emission and the fainter is the FL emission intensity.[34,35] For Pt-Q the FL emission around 510 nm becomes much stronger than the PH emission at ~740 nm. When the effective SOC in the polymer chain weakens, the PH emission from the TE weakens and the FL band from SE strengthens. Consequently we estimate that the SOC is strongest for Pt-1 and weakest for Pt-Q, as suggested by their spacer sizes in their chemical structure.

We first describe the obtained FICPO results in Pt-1 polymer using the difference between the R and L spectra at each *B* field, for both P and V bands (see Figs. 2a and 2b). We could observe derivative-like features that originate from the Zeeman splitting, ΔE between the R and L emission bands. To extract the central wavelength and the accurate emission intensity for the P and V bands, we fitted each original spectrum with Lorentzian-shape bands superpose on a linear response that represents the background spectrum. As a result it was possible to extract the R-L energy splitting, $\Delta E(B)=E_R-E_L$ as a function of *B* for the P and V bands, as shown in Figs. 2c and 2d (upper panels), respectively. Interestingly, ΔE is only ±0.2 meV for the P band at $B=\pm 17.5$ T, whereas it reaches ±2 meV for the V band, although both bands originate from the lowest lying TE state. Using the fitting procedure mentioned above, the FICPO values, CP(*B*) for the P and V bands were also extracted as presented in Figs. 2c and 2d (lower panels), respectively. As clearly seen both CP(*B*) responses are anti-symmetric respect to *B*,

namely CP(–*B*)=–CP(*B*); however the CP(*B*) responses for P and V bands are very different from each other. The CP(*B*) for the P band first increases from *B*=0 to 5 T (~2% at 5 T), followed by a decrease with *B,* reaching -4% at 17.5 T. In contrast, the CP(*B*) of the V band is monotonous with *B* up to approximately -2% at 17.5 T. The different field responses of the P and V bands show that the spin sublevels involved in these two PH bands that originate from their spin Hamiltonian differ substantially.

Following the same analysis procedure, we obtained the ΔE(*B*) and CP(*B*) responses of the FL, P and V bands in Pt-3 (Figs. 3a, 3b and 3c, respectively). Compared with those responses in Pt-1, the energy split and FICPO values of the PH bands are about 2-4 times smaller in the Pt-3 polymer. Surprisingly, a non-zero FICPO response was also measured for the FL band here; this is surprising when considering that the FL originates from the SE emission. This indicates that the strong SOC here mixes the TE and SE states. In comparison, the FL band of Pt-Q shows negligibly small FICPO response (Fig. 4a), whereas the obtained ΔE(*B*) of the PH band (Fig. 4b, upper panel) reaches a maximum of ~2 meV at *B*=10 T, and substantially decreases at *B*=17.5 T. Although the PH emission is quite weak here, its CP(*B*) response is larger than in the other two Pt-polymers; in fact the CP approaches ~50% at the highest field (Fig. 4b, lower panel). This indicates that the FL and PH emissions originate from SE and TE that do not mix when the SOC is relatively weak, a situation that increases FICPO of the TE state.

III. ANALYSIS AND DISCUSSION

In the following we show that the measured FICPO response in the Pt polymers can be properly analyzed to unravel the triplet exciton fine structure in these compounds. Photon absorption generates e-h pairs (or excitons) in the Pt-rich polymer chain, of which wave function is shared between the Pt negative paramagnetic ion (electronic configurations: neutral Pt-$5d^9 6s^1$, Pt^--$5d^9 6s^2$) and the positively charged organic spacers. Whereas the orbital angular momentum of the 5d orbital is L=2, the states that are responsible for circular polarized emission have magnetic quantum number of m=±1, and thus can be treated as coming from states of L=1. The low symmetry ligand field around the Pt ion splits the degenerate d-electron energy levels (Fig. 5a, left panel). Each level is spin degenerate that allows optical emission from an overall spin singlet exciton (unpolarized

emission). However the strong SOC further lifts the spin degeneracy, mixing orbital and spin characters in each level to allow optical emission from SE as well as from the TE. Upon the application of an external magnetic field, these levels are further split due to the Zeeman interaction (Fig. 5a, right panel), giving rise to asymmetry in the wave functions and unequal thermal populations with respect to the field direction. This asymmetry breaks the equivalence between R and L emission states which generates FICPO response in the Pt polymers.

The exciton electronic structure of the Pt-rich polymers was calculated before using the time-dependent density functional theory.[24,25] It was concluded that the emitting states are metal-to-ligand charge-transfer (MLCT) excitons, having π-π* character and efficient singlet-triplet intersystem crossing provided by the strong SOC from the intrachain Pt atoms. As for the PH emission, due to the SOC there exists a significant weight of spin singlet configuration in the TE states which allows optical dipole transitions to the ground state, S_0; which is spin singlet state with zero orbital angular momentum (L=0). We note that the π-π* character of the TE is in fact responsible for the strong optical transition to the S_0. In addition, the low structural symmetry of the Pt-rich polymer chain causes the SOC matrix to be anisotropic, that influences the FICPO responses. Consequently we examine the spin-orbit Hamiltonian of the TE using the following three-parameter expression,

$$H_{SOC} = \lambda \vec{L} \cdot \vec{S} + \vec{L} \cdot \tilde{\Lambda} \cdot \vec{S} \qquad (1)$$

where λ is the isotropic SOC parameter and $\tilde{\Lambda}$ is a 3x3 traceless symmetric matrix that accounts for the SOC anisotropy having two independent parameters: Λ_D and Λ_E. Note that the matrix $\tilde{\Lambda}$ contains the angular dependence of the SOC. As explained above we use for the TE L=1 that allows electric dipole optical transitions to S_0 (L=0).

The total TE spin Hamiltonian in a magnetic field B along the laboratory z-direction is thus written as,

$$H_{TEso} = H_{TE} + H_{SOC} - \mu_B g J_Z B \ , \qquad (2)$$

where the zero-field bare TE spin Hamiltonian is $H_{TE} = \vec{S} \cdot \tilde{D} \cdot \vec{S}$,[36,37] the angular dependent $\tilde{D}$ is the traditional ZFS traceless matrix of TE with D and E as the axially symmetric and asymmetric ZFS parameters, $J_z=L_z+S_z$ and g is the effective TE g-factor. We note, however that since we study the optical transition at low temperature (T=4 K) and high field (up to B=17.5 T), the effective g- factor in Eq. (2) is relevant only to the lowest thermally occupied spin sub-level.

We have calculated the wave functions and energy levels of the resulting 9x9 S⊗L spin Hamiltonian using Eq. (2) for various directions of the TE and SOC orientations. Figure 5b shows an example of the energy levels for g>0 and the parameters as shown in TABLE I. The relatively large SOC causes large splitting and mixes spin/orbital configuration among the levels. Optical transitions to S_0 (PH emission) with $(L_z,S_z)=(0,0)$ are allowed from all TE levels having non-zero (Lz,Sz)=(±1,0) weight, $P^{\pm}$. The emission intensity, I is described by $I^{R,L} \propto \sum_k P_k^{\pm} N_k \equiv \sum_k n_k^{R,L}$, where the summation is over all nine energy levels, where N_k is the thermal population of level k. Thereby the CP of the PH band, ρ_{PH} is given by,

$$\rho_{PH} = (I^R - I^L)/(I^R + I^L) = \sum_k (n_k^R - n_k^L) / \sum_k (n_k^R + n_k^L) . \qquad (3)$$

The calculated polarization weighted thermal populations, $n_k^{R,L}$, for the nine mixed spin/orbital sublevels (corresponding to the V band in Pt-1) at T=4 K are illustrated in Figs. 5c and 5d. Note that the population of $(L_z,S_z)=(+1,0)$ configuration at B field is equal to the population of $(L_z,S_z)=(-1,0)$ population at $-B$ field, thus generating an asymmetric CP(B) response, as obtained in the experiment. The red line through the data points in Fig. 2d (lower panel) is an actual fitting to the data using the model Hamiltonian of Eq. (2). The FICPO saturation at high field is caused by the diminishing population of the L_z=−1(+1) levels, as can be seen in the calculated polarization weighted thermal populations. We note that the positive (negative) CP(B) response for negative (positive) B is an indication of a positive (negative) g-factor. For Pt-3 and Pt-Q, the CP(B) response of the PH emission increases with B (Figs. 3c and 4b, lower panels), which originates from a negative g-factor, as seen for the red line fittings (see parameters in TABLE I).

We have also calculated the median photon energies, E_R and E_L of the R and L emission bands, by thermal-population-weighted averaging of the energies obtained from the Hamiltonian in Eq. (2). The calculated R-L energy splitting, $\Delta E(B)$ for the V band is plotted as red lines through the data in Figs. 2d, 3c, and 4b (upper panels) using the same parameters as for the CP(B) response fittings for Pt-1, Pt-3 and Pt-Q, respectively. The excellent fits obtained for both CP(B) and $\Delta E(B)$ responses validate the use of the ad-hoc Hamiltonian Eq. (2) to explain the TE emission and its FICPO response in the Pt polymers.

Recall that the CP(B) response for the P band in Pt-1 (Fig. 2c, lower panel) is different from that of the V band; it increases with B in the interval $0<B<5$ T, followed by a decrease with B in the interval $5<B<17.5$ T. The P band emission has been identified before as a 'super-PH' in which a pair of TEs emit coherently.[32] In this case, the CP(B) response of this band, which may be viewed as a TT pair should be different from that of a single TE because the main contribution to FICPO comes from the lowest thermally occupied levels (see Figs. 5c and 5d) having $L_z=\pm1$ and $S_z=0$. In a coupled TT pair, there are more thermally populated levels from which optical emission is possible. To account for the CP(B) response of the P-band in the PH emission described by TT pair, we write the zero-field Hamiltonian as:

$$H_{TT} = H_{TE1} + H_{TE2} + X\vec{S}_1 \cdot \vec{S}_2 \qquad (4)$$

where $H_{TE1,2}$ are the individual TE Hamiltonians with spins S_1, S_2 (given by Eq. (2)), and X is the TE-TE exchange coupling between the two TEs. Note that the full Hamiltonian is now written in Hilbert space dimension of 3x3x3=27. Also the effective g-factor for the TT pair excitation is different from that of TE because the spin configuration of the occupied levels is not the same in the two situations. In this case, the optical emission is allowed from $(L_z,S_z)=(\pm1,0)$, where $S_z=S_{1z}+S_{2z}$. To understand the FICPO response of the P-band we have solved the 27x27 Hamiltonian and calculated $\Delta E(B)$ and CP(B) for various angles between the B field and the principal axes of SOC and ZFS matrices. Figure 2c shows the fitting results using the parameters given in TABLE I, which clearly captures the significant slope change of CP(B) at ~5 T. It shows that this peculiar non-

monotonic field dependence of the P-band can be interpreted by involving all the sublevel populations that are responsible for the optical emission of T-T pair.

Another interesting experimental fact is the FICPO response of the FL emission in Pt-3 polymer. According to the density functional calculations,[24,25] the electron wave function of the emitting SE in Pt-3 (SE_1) is mostly centered on the Pt atom that introduces appreciable SOC, which renders the electric dipole allowed FL to be circularly polarized. For the FL band we consider a system composed of an electron and a hole (both having spin $S_1=S_2=½$) with anisotropic SOC with L=1 (Hilbert space dimensionality of 2x2x3=12). In this case the spin Hamiltonian in a magnetic field *B* along the laboratory z-direction is written as,

$$H_{FL} = H_{EX} + H_{SOC} - \mu_B g J_Z B \ , \qquad (5)$$

where H_{SOC} is given by Eq. (1), now with S=½ and L=1. The last term is the Zeeman interaction where $J_z=L_z+S_{1z}+S_{2z}$ with S_{1z}, $S_{2z}=\pm½$, $L_z=\pm1,0$ and g is the effective g-factor. H_{EX} is the anisotropic e-h exchange interaction that separates the singlet and triplet energy levels of the two spin ½ particles, for which we use an anisotropic exchange to account for the ZFS parameters of the excited TE level. The excited TE level (T_n) is close in energy to the SE_1 level, thus a significant near-resonant coupling SE_1-T_n is expected. Equation (5) therefore describes the 12 energy levels of SE and T_n coupled by the exchange and spin orbit interactions.

The procedure of calculating the FICPO response for the FL is similar to that for PH, namely we calculated the thermal-population-weighted median energy from the Hamiltonian given in Eq. (5), taking into account the thermal equilibrium populations of the states $(L_z,S_z)\equiv(L_z,S_{1z}+S_{2z})= (\pm1,0)$. The calculated FICPO response (red lines in Fig. 3a upper and lower panels) generally agrees with the experimental data for the FL band in Pt-3; the obtained fitting parameters for the exciton fine structure are given in TABLE I. The moderate CP fitting of the FICPO response for the FL emission is probably due to the fact that our model does not consider that the ultrafast FL emission in Pt-polymers occurs under extreme dynamic conditions, where thermal equilibrium is not reached.

IV. CONCLUSIONS

In summary, we have shown that the steady-state magneto-optical spectroscopy provides an effective method for studying the photoexcitation spin-related properties in Pt-rich π-conjugated polymers, where the strong SOC accelerates the spin relaxation and thus limits the use of other main-stream methods. By measuring the circularly polarized emission under high magnetic field we obtained important information about the fine structure of the excitons in these Pt polymers, such as the TE effective *g*-value, and the parameters related to the SOC and exchange interaction. Moreover, we found that the super-PH that we treat here as coming from TT pairs, and the FL from SE also have circular polarization properties at high field, which could be quantitatively modeled using appropriate Hamiltonians. The experimental results and the theoretical models represent a promising way to probe TE fine structure using magneto-optical measurements, and open the way towards future spin-related optoelectronic research in organic semiconductors.

ACKNOWLEDGMENTS

This work was supported by the National Science Foundation grant (DMR-1701427). The work at Technion was supported by the Israel Science Foundation (ISF 598/14). A portion of this work was performed at the National High Magnetic Field Laboratory in Tallahassee FL, which is supported by National Science Foundation Cooperative Agreement No. DMR-1157490 and the State of Florida.

(1) D. T. Pierce, and F. Meier, Photoemission of spin-polarized electrons from GaAs. Phys. Rev. B **13**, 5484 (1976).

(2) R. Kotlyar, T. L. Reinecke, M. Bayer, and A. Forchel, Zeeman spin splittings in semiconductor nanostructures, Phys. Rev. B **63**, 085310 (2001).

(3) M. Bayer, A. Kuther, A. Forchel, A. Gorbunov, V. B. Timofeev, F. Schäfer, J. P. Reithmaier, T. L. Reinecke, and S. N. Walck, Electron and Hole *g* Factors and Exchange Interaction from Studies of the Exciton Fine Structure in $In_{0.60}Ga_{0.40}As$ Quantum Dots, Phys. Rev. Lett. **82**, 1748-1751 (1999).

(4) M. Bayer, G. Ortner, O. Stern, A. Kuther, A. A. Gorbunov, A. Forchel, P. Hawrylak, S. Fafard, K. Hinzer, T. L. Reinecke, S. N. Walck, J. P. Reithmaier, F. Klopf, and F.

Schäfer, Fine structure of neutral and charged excitons in self-assembled In(Ga)As/(Al)GaAs quantum dots, Phys. Rev. B **65**, 195315 (2002).

(5) K. Kheng, R. T. Cox, D. A. My, F. Bassani, K. Saminadayar, and S. Tatarenko, Observation of negatively charged excitons X- in semiconductor quantum wells, Phys. Rev. Lett. **71**, 1752-1755 (1993).

(6) E. Blackwood, M. J. Snelling, R. T. Harley, S. R. Andrews, and C. T. B. Foxon, Exchange interaction of excitons in GaAs heterostructures, Phys. Rev. B **50**, 14246-14254 (1994).

(7) K. Nakamura, K. Ohya, and O. Arimoto, Magnetic field effects on the triplet excitons in β-ZnP_2, J. Lumin. **94**, 393-396 (2001).

(8) T. Tsuboi, and M. Tanigawa, Optical characteristics of PtOEP and $Ir(ppy)_3$ triplet-exciton materials for organic electroluminescence devices, Thin Solid Films **438**, 301-307 (2003).

(9) A. F. Rausch, and H. Yersin, Magnetic field effects on the phosphorescence of Pt(4,6-dFppy)(acac)–Tunability of the vibrational satellite structure, Chem. Phys. Lett. **484**, 261-265 (2010).

(10) M. Wohlgenannt, E. Ehrenfreund, and Z. V. Vardeny, Photophysics of Molecular Materials, Wiley-VCH Verlag GmbH & Co. KGaA, 183-259 (2006).

(11) H. Yersin, E. Gallhuber, and G. Hensler, and D. Schweitzer, Zero-field splittings of the two lowest excited electronic states in crystalline $[Ru(bpy)_3]X_2$ with X= PF_6, ClO_4. Chem. Phys. Lett. **161**, 315-320 (1989).

(12) C. V. Diaconu, E. R. Batista, R. L. Martin, D. L. Smith, B. K. Crone, S. A. Crooker, D. L. Smith's, Circularly polarized photoluminescence from platinum porphyrins in organic hosts: Magnetic field and temperature dependence, J. Appl. Phys. **109**, 073513 (2011).

(13) E. Gallhuber, G. Hensler, and H. Yersin, Magnetic-field effects in the low-temperature polarized emission and absorption spectra of single-crystal $[Ru(bpy)_3](PF_6)_2$, J. Am. Chem. Soc. **109**, 4818-4822 (1987).

(14) S. Polosan, I. C. Radu, and T. Tsuboi, Photoluminescence and magnetic circular dichroism of $IrQ(ppy)_2$-5Cl, J. Lumin. **132**, 998-1002 (2012).

(15) M. Grell, and D. D. C. Bradley, Polarized Luminescence from Oriented Molecular Materials, Adv. Mater. **11**, 895-905 (1999).

(16) E. M. Sánchez-Carnerero, A. R. Agarrabeitia, F. Moreno, B. L. Maroto, G. Muller, M. J. Ortiz, and S.de la Moya, Circularly Polarized Luminescence from Simple Organic Molecules, Chem. Euro. J. **21**, 13488-13500 (2015).

(17) J. A. Schauerte, D. G. Steel, and A. Gafni, Time-resolved circularly polarized protein phosphorescence, Proc. Natl. Acad. Sci. U.S.A. **89**, 10154-10158 (1992).

(18) E. Gussakovsky, Reviews in Fluorescence, C. D. Geddes, Ed. Springer New York, New York, NY, 425-459 (2008).

(19) D. Yang, P. Duan, L. Zhang, and M. Liu, Chirality and energy transfer amplified circularly polarized luminescence in composite nanohelix, Nat. Commun. **8**, 15727 (2017).

(20) R. Naaman, and D. H. Waldeck, Spintronics and Chirality: Spin Selectivity in Electron Transport Through Chiral Molecules, Annu. Rev. Phys. Chem. **66**, 263-281 (2015).

(21) R. C. Evans, P. Douglas, and C. J. Winscom, Coordination complexes exhibiting room-temperature phosphorescence: evaluation of their suitability as triplet emitters in organic light emitting diodes, Coord. Chem. Rev. **250**, 2093-2126 (2006).

(22) T. D. Nguyen, Y. Sheng, J. Rybicki, G. Veeraraghavan, and M. Wohlgenannt, Magnetoresistance in π-conjugated organic sandwich devices with varying hyperfine and spin-orbit coupling strengths, and varying dopant concentrations, J. Mater. Chem. **17**, 1995-2001 (2007).

(23) Y. Wu, Z. Xu, B. Hu, and J. Y. Howe, Tuning magnetoresistance and magnetic-field-dependent electroluminescence through mixing a strong-spin-orbital-coupling molecule and a weak-spin-orbital-coupling polymer, Phys. Rev. B **75**, 035214 (2007).

(24) A. Kohler, J. S. Wilson, R. H. Friend, M. K. Al-Suti, M. S. Khan, A. Gerhard, and H. Bassler, The singlet–triplet energy gap in organic and Pt-containing phenylene ethynylene polymers and monomers, J. Chem. Phys. **116**, 9457-9463 (2002).

(25) C. X. Sheng, S. Singh, A. Gambetta, T. Drori, M. Tong, S. Tretiak, and Z. V. Vardeny, Ultrafast intersystem-crossing in platinum containing p-conjugated polymers with tunable spin-orbit coupling, Sci. Rep. **3**, 2653 (2013).

(26) D. Sun, K. J. Van Schooten, M. Kavand, H. Malissa, C. Zhang, M. Groesbeck, C. Boehme, and Z. V. Vardeny, Inverse spin Hall effect from pulsed spin current in organic semiconductors with tunable spin-orbit coupling, Nat. Mater. **15**, 863-869 (2016).

(27) W. J. Finkenzeller, T. Hofbeck, M. E. Thompson, and H. Yersin, Triplet state properties of the OLED emitter $Ir(btp)_2(acac)$: characterization by site-selective spectroscopy and application of high magnetic fields, Inorg. Chem. **46**, 5076-5083 (2007).

(28) H. Yu, X. Cui, X. Xu, and W. Yao, Valley excitons in two-dimensional semiconductors, Nat. Sci. Rev. **2**, 57-70 (2015).

(29) G. Aivazian, Z. Gong, A. M. Jones, R. Chu, J. Yan, D. Mandrus, C. Zhang, D. H. Cobden, W. M. Yao, and X. Xu, Magnetic control of valley pseudospin in monolayer WSe_2, Nat. Phys. **11**, 148-152 (2015).

(30) A. Srivastava, M. Sidler, A. Allain, D. Lembke, A. Kis, and A. Imamoglu, Valley Zeeman effect in elementary optical excitations of monolayer WSe_2, Nat. Phys. **11**, 141-147 (2015).

(31) C. Zhang, D. Sun, C. X. Sheng, Y. X. Zhai, K. Mielczarek, A. Zakhidov, and Z. V. Vardeny, Magnetic field effects in hybrid perovskite devices, Nat. Phys. **11**, 427-434 (2015).

(32) B. Khachatryan, T. D. Nguyen, Z. V. Vardeny, and E. Ehrenfreund, Phosphorescence superradiance in a Pt-containing π-conjugated polymer, Phys. Rev. B **86**, 195203 (2012).

(33) C. Zhang, D. Sun, Z. G. Yu, C. X. Sheng, S. McGill, D. Semenov, and Z. V. Vardeny, Field-induced spin splitting and anomalous photoluminescence circular

polarization in $CH_3NH_3PbI_3$ films at high magnetic field, Phys. Rev. B **97**, 134412 (2018).

(34) P. M. L. Blok, H. Jacobs, and H. P. J. M. Dekkers, Circular polarization of the phosphorescence of α,β-Enones: effect of triplet-triplet coupling. Evidence for nondistorted 3ππ* states, J. Am. Chem. Soc. **113**, 794-801 (1991).

(35) C. Yang, Z. V. Vardeny, A. Kohler, M. Wohlgenannt, M. K. Alsuti, and M. S. Khan, Spectroscopic study of spin-dependent exciton formation rates in π-conjugated semiconductors: Comparison with electroluminescence techniques, Phys. Rev. B **70**, 241202(R) (2004).

(36) E. Ehrenfreund, and Z. V. Vardeny, Effects of magnetic field on conductance and electroluminescence in organic devices, Isr. J. Chem. **52**, 552-562 (2012).

(37) R. E. Merrifield, Magnetic effects on triplet exciton interactions. Pure Appl. Chem. **27**, 481-498 (1971).

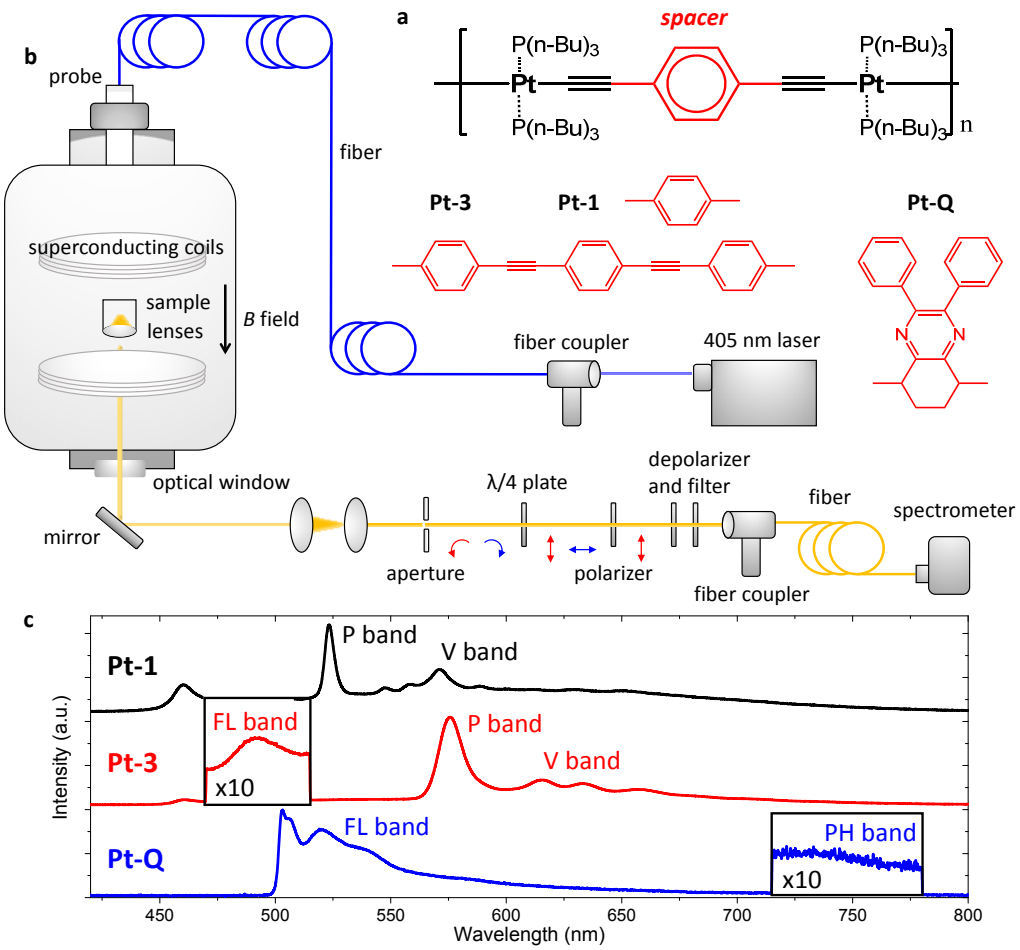

FIG. 1. (a) Chemical structures of the Pt-rich polymers with various spacers (Pt-1, Pt-3 and Pt-Q as denoted). (b) Experimental setup for measuring circularly polarized emission at high field and low temperature. (c) The emission spectra of Pt-1 (black line), Pt-3 (red line) and Pt-Q (blue line) at 4 K that show various bands including the fluorescence (FL) band and the phosphorescence (PH) emission (P band and V band). The emission around 460 nm originates from the long pass optical filter.

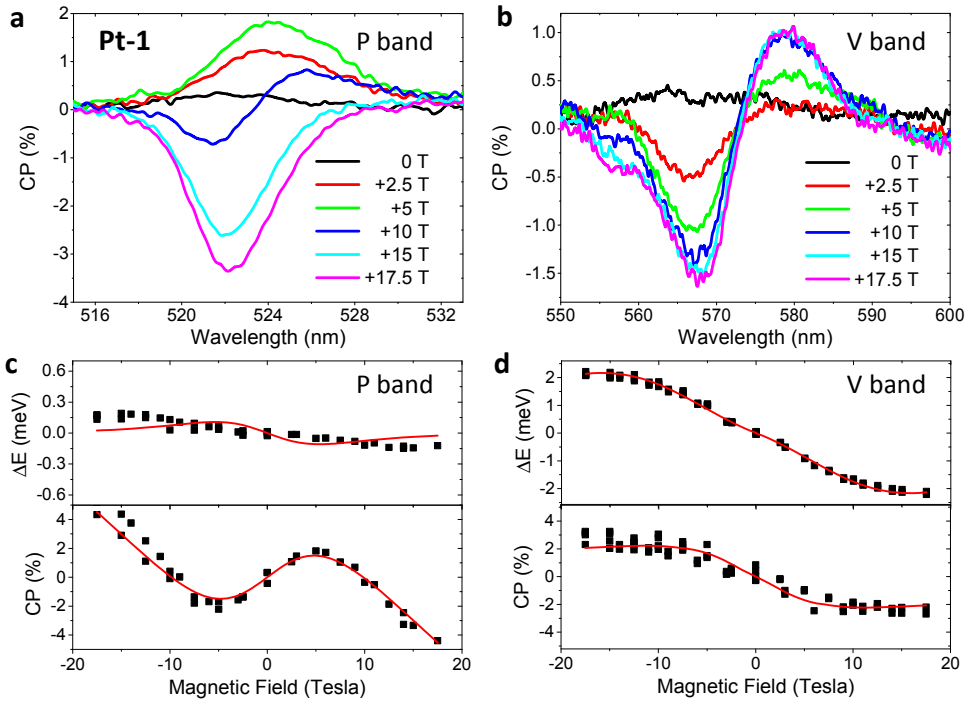

FIG. 2. The circular polarization (CP) spectra, CP(λ) for (a) the P band and (b) the V band of the PH emission in Pt-1 film, measured at 4K in the field range of ±17.5 T. The extracted R-L energy split, ΔE(*B*) (upper panels) and the FICPO response, CP(*B*) (lower panels) of the P band (c) and V band (d). The red lines through the data points are fits using the model described in the text, with parameters given in TABLE I.

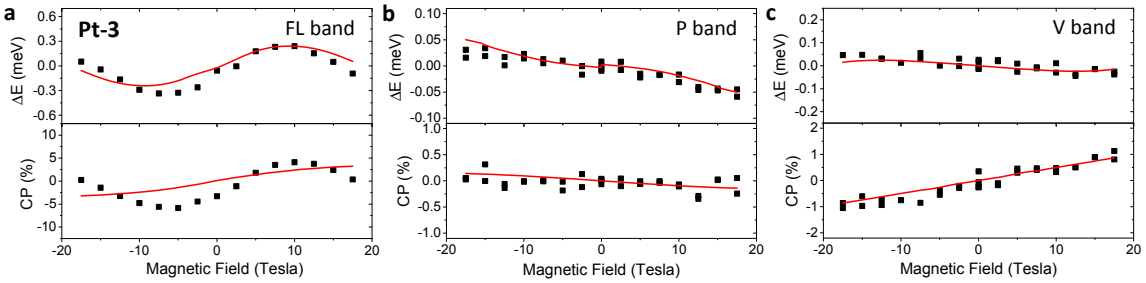

FIG. 3. The R-L energy split, ΔE(*B*) (upper panels) and the FICPO response, CP(*B*) (lower panels) for the various Pt-3 emission bands: (a) the FL band, (b) the PH P-band, and (c) the PH V-band. The red lines through the data points are fits using the model described in the text with parameters given in TABLE I.

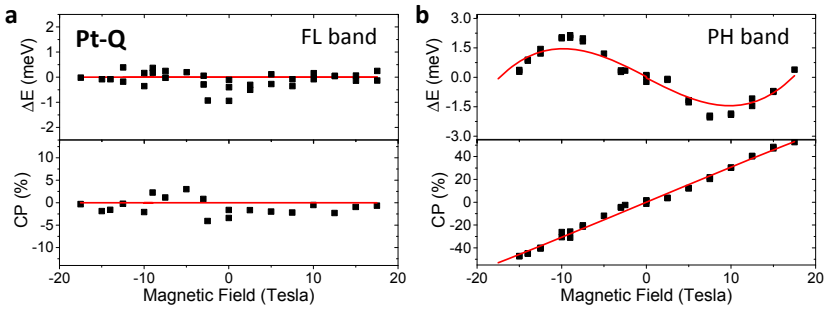

FIG. 4. The R-L energy shift, ΔE(*B*) and FICPO response, CP(*B*) for (a) the FL band and (b) the PH band in Pt-Q. The red lines through the data points are fits using the model described in the text with parameters given in TABLE I.

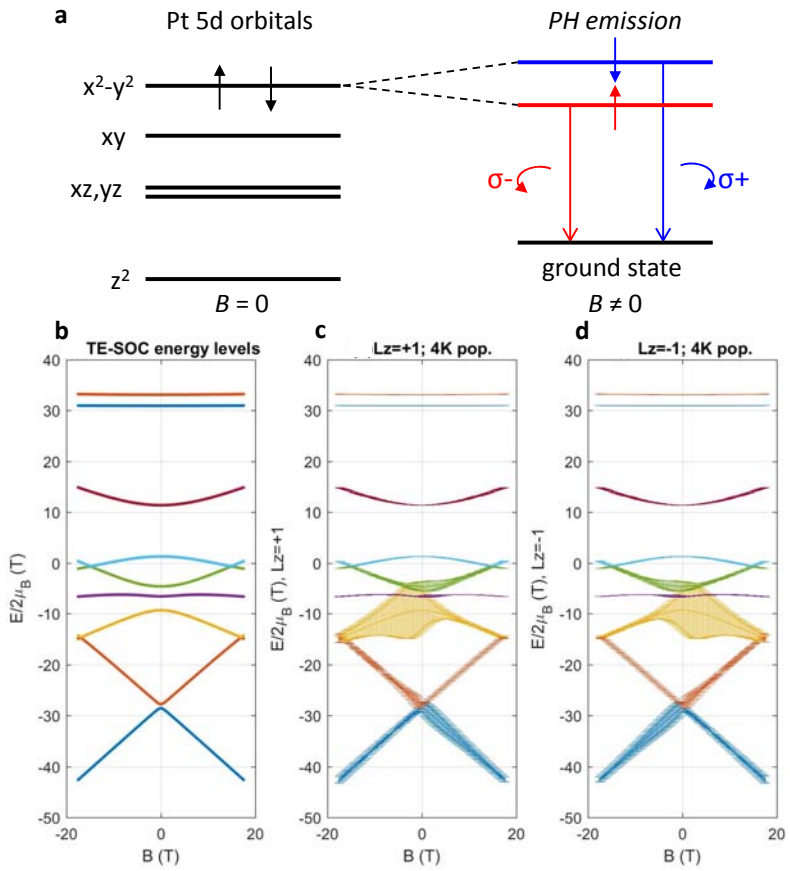

FIG. 5. (a) Schematic illustration of the d-electron levels of the Pt atom in Pt-rich polymers by taking the ligand field and SOC into account. Left column: the orbital and spin splitting in a planar crystal field with SOC. Right column: the Zeeman splitting of the upper electron level that yields circular polarized emission. (b) Calculated TE-SOC energy levels subjected to external field based on the Hamiltonian given in Eq. (2) using the fitting parameters for the Pt-1 V band (see TABLE I). The calculated (c) R and (d) L polarization weighted thermal populations at T=4 K are displayed as vertical bars on the energy level scheme shown in (b).

TABLE I. The best fitting parameters for the model calculation of FICPO response in Pt-rich polymers. The ZFS columns are the zero-field splitting energies for TE; the SOC columns give the anisotropic spin-orbit coupling parameters; the exchange columns give the TE-TE isotropic exchange coupling for the P band and the e-h anisotropic exchange coupling for the FL band.

	ZFS (meV)		SOC (meV)			*g* factor	exchange (meV)		
	D	E	iso	axial	asym		iso	axial	asym
Pt-1, P band	-1.5	0.11	-0.31	-1.4	-0.72	0.5	-0.27	--	--
Pt-1, V band	-0.053	-0.62	-0.65	2.6	1.8	0.85	--	--	--
Pt-3, FL band	--	--	-0.048	0.95	1.6	-0.93	-0.41	0.20	0.23
Pt-3, P band	-1.4	0.16	-0.64	-0.13	-0.31	0.39	-0.67	--	--
Pt-3, V band	-0.12	-0.12	-0.20	-0.47	1.74	-0.1	--	--	--
Pt-Q, PH band	-0.019	-0.60	-0.29	0.41	1.6	-0.13	--	--	--